Inverse dielectric function of a lateral quantum wire superlattice parallel to the interface of a plasma-like semiconductor

Norman J. M. Horing[1] and L. Y. Chen[2]
[1]*Department of Physics and Engineering, Physics, Stevens Institute of Technology, Hoboken, New Jersey 07030, USA*
[2]*Department of Physics, University of Texas at San Antonio, San Antonio, Texas 78249, USA*
(Received 19 May 2006; revised manuscript received 14 September 2006; published 27 November 2006)

The dynamic, nonlocal, and spatially inhomogeneous polarizability and dielectric function are discussed in this paper for a Coulomb-coupled system of a periodic lateral superlattice array of one-dimensional quantum wire plasmas in the vicinity of a semi-infinite bulk plasma. The space-time matrix inverse of the dielectric function, i.e., the dynamic, nonlocal, inhomogeneous screening function of this system, is determined analytically here in closed form solving a random-phase-approximation type integral equation in position representation. We treat both cases wherein the lateral quantum wire superlattice is outside the semi-infinite plasma as well as inside. We also determine the exact coupled plasmon dispersion relation for the combined system for both the "outside" and "inside" cases: in this, we examine the band and gap structure of the spectrum due to periodicity of the quantum wire superlattice in the first Brillouin zone as a function of reciprocal-lattice wave number p, and also as a function of wave vector q_x along the wire direction of full translational invariance. Furthermore, we analyze the spectrum of the combined system as a function of the period of the superlattice, showing that the detailed variation of the band-structure spectrum and gaps reflects on the period of the superlattice, opening the possibility of using surface plasmon resonance as a mechanism for optical sensing of nanostructure geometry. We also determine the dependence of the spectrum on distance of the superlattice from the bounding surface of the semi-infinite plasma, for both outside and inside cases. In the outside case, we show that at large distances the surface plasmon decouples from the superlattice plasmon band, while for short distances the two are fully coupled. For the inside case, they are similarly fully coupled for short distances, but for large distances, the surface plasmon decouples while the wire-superlattice plasmon band couples to the *bulk* plasmon deep in the semi-infinite medium.

DOI: 10.1103/PhysRevB.74.195336 PACS number(s): 73.20.Mf, 73.21.Hb, 73.21.Cd

I. INTRODUCTION

Surface plasmon resonance, which has been well understood for about half a century,[1–3] has come to play an important role in chemical sensing and biotechnological measurements over the past 20 years.[4–16] Its utility is rooted in the fact that it is based on boundary conditions, so that the surface plasmon spectrum sensitively reflects features of an adsorbate material introduced outside the surface. In this paper, we focus attention on the interaction of surface plasmons with those of a lateral quantum wire-like superlattice[17–20] structure parallel to the surface. The coupling of these modes, and associated modifications of the spectrum, change the joint optical response and reflectivity of the combined system in a way that provides detailed information about the wire-like superlattice. Such information includes the normal-mode frequency spectrum of the superlattice itself, and its geometric parameters, a point that we emphasize here as a step in the determination of the geometric structure of a nanomolecular architecture in the vicinity of a surface.

Our analysis of the coupled spectrum is presented in terms of the inverse dielectric function ("screening" function) of the combined system composed of a semi-infinite plasma and a lateral quantum-wire-like superlattice plasma, with Coulombic coupling between the two systems as well as within each individually. The frequency poles of this function provide the coupled plasmon frequency spectrum, and the residues at these frequency poles describe the oscillator strengths (excitation amplitudes) with which they respond to excitation. In Sec. II we formulate the integral equation for the screening function of the combined system, employing the known screening function for the semi-infinite plasma alone. In Sec. III the polarizability of the lateral quantum wire superlattice, which is the kernel of the integral equation, is described in detail. The integral equation for the combined system screening function is solved explicitly in Sec. IV, and the coupled mode spectrum is examined in Sec. V. Concluding remarks are presented in Sec. VI.

II. FORMULATION OF THE INTEGRAL EQUATION FOR THE SCREENING FUNCTION OF A LATERAL QUANTUM WIRE SUPERLATTICE COUPLED TO A SEMI-INFINITE SEMICONDUCTOR PLASMA

In this section we formulate the integral equation involved in the determination of the spatially inhomogeneous, nonlocal frequency-dependent screening function of a periodic lateral quantum wire superlattice parallel to the surface of a semi-infinite plasma at a distance $|z_0|$ from the interface. This screening function, $K(1,2)$, $[1=\vec{r}_1,t_1]$ is the space-time matrix inverse of the direct dielectric function $\epsilon(1,2)$, written explicitly as

$$\int d^4 3\,\epsilon(1,3)K(3,2) = \delta^{(4)}(1-2) = \delta(t_1-t_2)\delta^{(3)}(\vec{r}_1-\vec{r}_2), \tag{1}$$

or, in space-time matrix notation,

$$\epsilon K = 1. \tag{2}$$

Considering a planar interface and quantum wires in a parallel planar arrangement in the x direction, we employ an x-spatial Fourier transform ($x_1 - x_3 \to q_x$) as well as a time transform ($t_1 - t_3 \to \omega$) to write the inversion condition of Eq. (1) as a y-z matrix inversion. The frequency poles of $K(y_3, z_3; y_2, z_2; q_x, \omega)$ define the coupled plasmons of the lateral wire superlattice and semi-infinite medium, and the residues at these frequencies provide the relative excitation amplitudes (oscillator strengths) of the coupled modes. The spectrum of these Coulomb coupled electrostatic oscillations will be examined here in regard to its dependencies on q_x and z_0, the distance of the plane of the wires from the interface bearing semi-infinite surface plasmons in interaction with the wire superlattice plasmons. Furthermore, the wires are located periodically in the y direction with period a, giving rise to band structure in the spectrum, and we also examine its dependence on period and on the conjugate Fourier series variable p in the first Brillouin zone, $-\pi/a \leqslant p \leqslant \pi/a$.

In analyzing this system, we will add the polarizabilities of the constituent parts, namely α_{semi} of the semi-infinite medium and α_{SL} of the lateral quantum wire superlattice, with

$$\epsilon = 1 + \alpha_{semi} + \alpha_{SL} = \epsilon_{semi} + \alpha_{SL}. \tag{3}$$

This simple addition of polarizabilities is valid provided that electron states in the quantum wire lattice subbands do not significantly overlap the electron states of the semi-infinite bulk plasma.[21] The inversion relation then takes the form

$$(\epsilon_{semi} + \alpha_{SL})K = 1. \tag{4}$$

Acting from the left with K_{semi} (which satisfies $K_{semi}\epsilon_{semi}=1$), we have

$$K = K_{semi} - K_{semi}\alpha_{SL}K. \tag{5}$$

This is the integral equation that we analyze to solve for the joint screening function K of the combined parts of the whole system:

$$\begin{aligned} K(y_1, z_1; y_2, z_2; p_x, \omega) = {} & K_{semi}(y_1, z_1; y_2, z_2; p_x, \omega) \\ & - \int dz_4 \int dy_4 \int dz_3 \int dy_3 \\ & \times K_{semi}(y_1, z_1; y_4, z_4; p_x, \omega) \\ & \times \alpha_{SL}(y_4, z_4; y_3, z_3; p_x, \omega) \\ & \times K(y_3, z_3; y_2, z_2, p_x, \omega). \end{aligned} \tag{6}$$

It is equivalent to the random-phase approximation (RPA) integral equation in the absence of overlap as cited above.[21]

In earlier work[22,23] we determined the screening function of the semi-infinite semiconductor medium occupying the half space $z>0$ having a dynamic (but local) dielectric function, $\epsilon=\epsilon(\omega)$, with the other half space $z<0$ having dielectric function ϵ'. The result for K_{semi}, expressed in terms of the $x_1 - x_2 \to q_x$ spatial Fourier transform in the direction of translational invariance and ω-frequency variables (suppressed), is given by

$$\begin{aligned} K_{semi}(y_1, z_1; y_2, z_2) = {} & \frac{1}{\eta_+(z_1)}\delta(y_1 - y_2)\delta(z_1 - z_2) \\ & - \delta(z_2)\Gamma\frac{\eta_-(z_1)}{\eta_+(z_1)}\int \frac{dq_y}{2\pi} e^{iq_y(y_1 - y_2)} e^{-|z_1|\sqrt{q_x^2 + q_y^2}}, \end{aligned} \tag{7}$$

where Γ is the image strength factor,

$$\Gamma = \frac{\epsilon' - \epsilon}{\epsilon' + \epsilon}, \tag{8}$$

and ($\theta(z)$ is the Heaviside unit step function)

$$\eta_-(z) = \theta(z) - \theta(-z); \quad \eta_+(z) = \epsilon\theta(z) + \epsilon'\theta(-z). \tag{9}$$

To accommodate the study of interaction with quantum wires in the x direction the q_y integration is carried out, yielding

$$\begin{aligned} K_{semi}(y_1, z_1; y_2, z_2) = {} & \frac{1}{\eta_+(z_1)}\delta(y_1 - y_2)\delta(z_1 - z_2) \\ & - \delta(z_2)\Gamma\left(\frac{|q_x||z_1|}{\pi}\right)\frac{\eta_-(z_1)}{\eta_+(z_1)} \\ & \times \frac{K_1(|q_x|\sqrt{(y_1 - y_2)^2 + z_1^2})}{\sqrt{(y_1 - y_2)^2 + z_1^2}}, \end{aligned} \tag{10}$$

where $K_1(z)$ is the MacDonald function of order 1.

III. DIELECTRIC POLARIZABILITY OF LATERAL QUANTUM WIRE SUPERLATTICE

Taking the lateral periodic superlattice of identical quantum wires to be parallel to the x direction and equally spaced at $y=na$ ($n=-\infty, \ldots -1, 0, 1, \ldots, \infty$) on the plane $z=z_0$, its polarizability may be written (in the absence of wave function overlap between the wires) as

$$\alpha_{wires}(y_1, z_1; y_3, z_3) = \sum_{n=-\infty}^{\infty} \alpha_n(y_1, z_1; y_3, z_3), \tag{11}$$

and assuming no tunneling or interwire transitions,

$$\begin{aligned} \alpha_n(y_1, z_1; y_3, z_3) = {} & -\int dy_2' dz_2' v(y_1 - y_2', z_1 - z_2') \\ & \times R^{(n)}(y_2', z_2'; y_3, z_3), \end{aligned} \tag{12}$$

where v is the Coulomb potential and $R^{(n)}(y_2', z_2'; y_3, z_3)$ is the RPA ring diagram of the n^{th} wire, both in q_x-ω representation. The one-dimensional q_x-Fourier transform of the Coulomb potential is

$$\begin{aligned} & v(y_1 - y_2'; z_1 - z_2'; q_x, \omega) \\ & \quad = 2e^2 K_0(|q_x|[(y_1 - y_2')^2 + (z_1 - z_2')^2]^{1/2}), \end{aligned} \tag{13}$$

where $K_0(z)$ is the MacDonald function of order 0. The individual wire ring diagrams may be written in terms of single wire y-z subband eigenfunctions denoted by α, β as

$$R^{(n)}(y_1,z_1;y_2,z_2)=\sum_{\alpha,\beta}R^{(n)}_{\alpha\beta}(q_x,\omega)\Phi^n_{\alpha\beta}(y_1,z_1;y_2,z_2), \quad (14)$$

where we assume a single populated y subband, $\chi(y_1)$, and the possibility of several z subbands, $\xi^{(n)}_\alpha(z)$, which are real, with discrete energy eigenvalues $E_{\alpha n}$ and $\phi^{(n)}_\alpha(y_1,z_1)=\chi(z_1)\xi^{(n)}_\alpha(y_1)$ with

$$R^{(n)}_{\alpha\beta}(q_x,\omega)=2\int\frac{dq'_x}{2\pi}\frac{f_0(\epsilon_{q'_x-q_x}+E_{\beta n})-f_0(\epsilon_{q'_x}+E_{\alpha n})}{\omega+\epsilon_{q'_x-q_x}-\epsilon_{q'_x}+(E_{\beta n}-E_{\alpha n}+i0^+)}, \quad (15)$$

and (f_0 is the Fermi distribution)

$$\Phi^n_{\alpha\beta}(y_1,z_1;y_2,z_2)=\phi^{(n)}_\alpha(y_1,z_1)\phi^{(n)}_\alpha(y_2,z_2)\times\phi^{(n)}_\beta(y_1,z_1)\phi^{(n)}_\beta(y_2,z_2). \quad (16)$$

(The factor of 2 comes from the spin sum over electron states; $\epsilon_{q_x}=\hbar^2q_x^2/2m$.) In summary,

$$\alpha_{wires}(y_1,z_1;y_3,z_3)=-2e^2\sum_{\alpha,\beta}\sum_{n=-\infty}^{\infty}R^{(n)}_{\alpha\beta}(q_x,\omega)V^{(n)}_{\alpha\beta}(y_1,z_1)\times\phi^{(n)}_\alpha(y_3,z_3)\phi^{(n)}_\beta(y_3,z_3), \quad (17)$$

where

$$V^{(n)}_{\alpha\beta}(y_1,z_1)=\int dy'_2\int dz'_2\phi^{(n)}_\alpha(y'_2,z'_2)\times K_0(|q_x|[(y_1-y'_2)^2+(z_1-z'_2)^2]^{1/2})\phi^{(n)}_\beta(y'_2,z'_2). \quad (18)$$

Alternatively, taking the wires to be extremely narrow, we have $|\chi(z)|^2=\delta(z-z_0)$ and $|\phi^{(n)}_\alpha(y)|^2=\delta(y-na)$ (normalization), and neglecting intersubband transitions that involve relatively large energy denominators (with $E_\alpha\neq E_\beta$) in $R^{(n)}_\alpha(q_x,\omega)$, we write $R^{(n)}_{\alpha\beta}(q_x,\omega)=R^{(n)}_\alpha(q_x,\omega)\delta_{\alpha\beta}$, obtaining (as the wires are identical, $R^{(n)}_\alpha\to R_\alpha$ actually has no dependence on the wire index n)

$$\alpha_{wires}(y_1,z_1;y_3,z_3)=-2e^2\delta(z_3-z_0)\sum_n A^{(n)}(y_1,z_1)\delta(y_3-na), \quad (19)$$

where

$$A^{(n)}(y_1z_1)=K_0(|q_x|[(y_1-na)^2+(z_1-z_0)^2]^{1/2})\sum_\alpha R_\alpha(q_x,\omega). \quad (20)$$

Substituting Eqs. (19) and (20) into the integral equation (6), we obtain (suppressing q_x,ω)

$$K(y_1,z_1;y_2,z_2)=K_{semi}(y_1,z_1;y_2,z_2)+2e^2\sum_n C(y_1-na;z_1)K(na,z_0;y_2,z_2), \quad (21)$$

where (put $Y=y_4-na$ below)

$$C(y_1-na;z_1)=\left(\sum_\alpha R_\alpha(q_x,\omega)\right)\int dz_4\int dy_4\times K_{semi}(y_1-y_4;z_1,z_4)\times K_0(|q_x|[(y_4-na)^2+(z_4-z_0)^2]^{1/2})$$
$$=\left(\sum_\alpha R_\alpha(q_x,\omega)\right)\int dz_4\int d\mathrm{Y}\times K_{semi}(y_1-na-\mathrm{Y};z_1,z_4)\times K_0(|q_z|[\mathrm{Y}^2+(z_4-z_0)^2]^{1/2}). \quad (22)$$

IV. SCREENING FUNCTION OF THE COMBINED SYSTEM: DISPERSION RELATION AND LATERAL PLASMON BAND STRUCTURE

To solve Eq. (21) for the screening function $K(y_1,z_1;y_2,z_2)$ it is necessary to determine $K(na,z_0;y_2,z_2)$ on the right-hand side. Therefore we set $y_1=ma$, $z_1=z_0$ on the left-hand side, obtaining

$$K\ (ma,z_0;y_2,z_2)]=K_{semi}(ma,z_0;y_2,z_2)+2e^2\sum_{n=-\infty}^{\infty}C(ma-na;z_0)\times K(na,z_0;y_2,z_2). \quad (23)$$

Considering the lattice translational symmetry due to periodicity in the y direction, we employ a Fourier series analysis as in earlier work.[24] Suppressing the explicit appearance of y_2, z_2, and z_0 for the moment, we write

$$K(ma)=K_{semi}(ma)+2e^2\sum_{n=-\infty}^{\infty}C(ma-na)K(na) \quad (24)$$

and

$$K(ma)=\frac{a}{2\pi}\int_{-\pi/a}^{\pi/a}dpe^{-2pma}\tilde{K}(p);\quad \tilde{K}(p)=\sum_{r=-\infty}^{\infty}K(ra)e^{ipra}, \quad (25)$$

with

$$C(ma-na)=\frac{a}{2\pi}\int_{-\pi/a}^{\pi/a}dpe^{-ip(ma-na)}\tilde{C}(p). \quad (26)$$

The use of the Poisson sum formula in the form

$$\sum_{n=-\infty}^{\infty}e^{i(p-p')na}=\frac{2\pi}{a}\sum_{n=-\infty}^{\infty}\delta\left(p-p'-\frac{2\pi n}{a}\right), \quad (27)$$

in which only the $\delta(p-p')$ term on the right-hand side contributes in the fundamental interval, $-\frac{\pi}{a}\leqslant p\leqslant\frac{\pi}{a}$, yields

$$\tilde{K}(p)=\frac{\tilde{K}_{semi}(p)}{1-2e^2\tilde{C}(p)}, \quad (28)$$

with the result

$$K(y_1,z_1;y_2,z_2) = K_{semi}(y_1,z_1;y_2,z_2) + 2e^2 \sum_{n=-\infty}^{\infty} C(y_1 - na;z_1) \times \frac{a}{2\pi}\int_{-\pi/a}^{\pi/a} dp e^{-ipna} \frac{\tilde{K}_{semi}(p,z_0;y_2,z_2)}{1 - 2e^2 \sum_{r=-\infty}^{\infty} e^{ipra} C(ra,z_0)}, \quad (29)$$

where

$$\tilde{K}_{semi}(p,z_0;y_2,z_2) = \sum_{r=-\infty}^{\infty} e^{ipra} K_{\text{semi}}(ra,z_0;y_2,z_2), \quad (30)$$

and $K_{semi}(ra,z_0;y_2,z_2)$ is given by Eq. (10) with $C(y_1,z_0)$ given by Eq. (22).

The dispersion relation for the plasmons related to the presence of the lateral superlattice at distance z_0 from the interface is given by

$$1 - 2e^2 \sum_{r=-\infty}^{\infty} e^{irpa} C(ra,z_0) = 0. \quad (31)$$

To proceed, we evaluate $C(ra,z_0)$ using Eqs. (22) and (7) for K_{semi}, obtaining

$$\frac{\sum_{r=-\infty}^{\infty} e^{irap} C(ra,z_0)}{\sum_{\alpha} R_\alpha(q_x,\omega)} = \frac{1}{\eta_+(z_0)} \sum_{r=-\infty}^{\infty} e^{irap} K_0(|rq_x a|) - \Gamma \frac{\eta_-(z_0)}{\eta_+(z_0)} \times \int dY \int \frac{dq_y}{2\pi} e^{-iq_y Y} e^{-|z_0|\sqrt{q_x^2+q_y^2}} \times K_0(|q_x|[Y^2+z_0^2]^{1/2}) \sum_{r=-\infty}^{\infty} e^{ira(p+q_y)}. \quad (32)$$

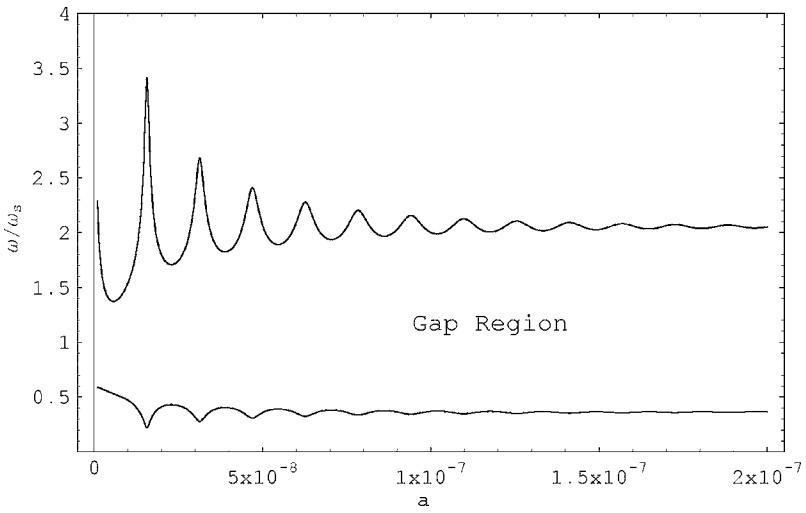

FIG. 2. $\omega_\pm/\omega_s$ as functions of a (m) for $z_0=-1$ nm, $p=4\times10^8$/m, $q_x=0.1q_F$.

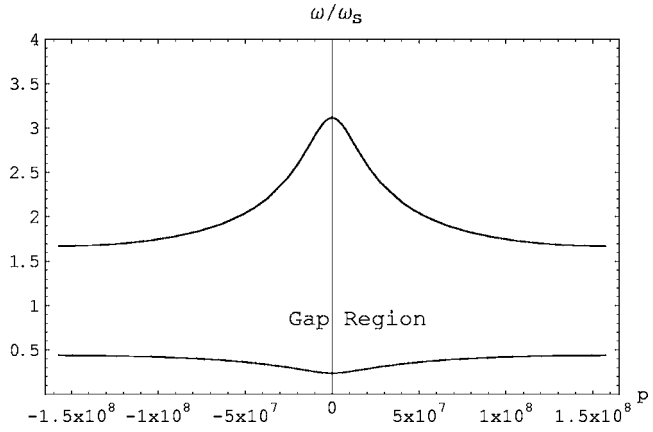

FIG. 1. $\omega_\pm/\omega_s$ as functions of p (1/m) for $z_0=-1$ nm, $a=20$ nm, $q_x=0.1q_F$.

Again invoking the Poisson sum rule, Eq. (27) and carrying out the q_y integration, we have

$$\frac{\sum_{r=-\infty}^{\infty} e^{irap} C(ra,z_0)}{\sum_{\alpha} R_\alpha(q_x,\omega)} = \frac{1}{\eta_+(z_0)} \sum_{r=-\infty}^{\infty} e^{irap} K_0(|rq_x a|) - \Gamma \frac{\eta_-(z_0)}{\eta_+(z_0)} \sum_{n=-\infty}^{\infty} e^{-|z_0|\sqrt{q_x^2+(2\pi n/a-p)^2}} \times \int_{-\infty}^{\infty} dY e^{iY(p-2\pi n/a)} K_0(|q_x|[Y^2+z_0^2]^{1/2}). \quad (33)$$

The Y integral yields an elementary function,[25] and the resulting dispersion relation is given by

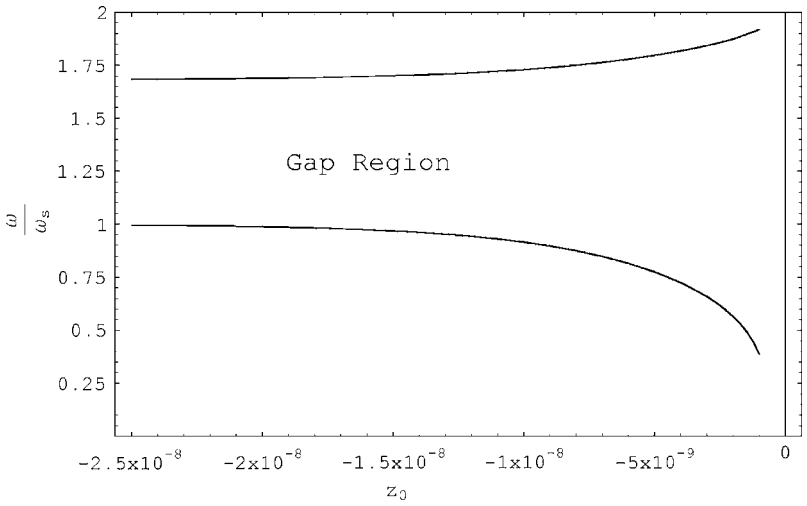

FIG. 3. $\omega_{\pm}/\omega_s$ as functions of negative z_0 (m) for $a=10$ nm, $p=10^8/\mathrm{m}$, $q_x=0.1q_F$.

$$1 = 2e^2\left(\sum_{\alpha} R_{\alpha}(q_x,\omega)\right)\left\{\frac{1}{\eta_+(z_o)}\sum_{r=-\infty}^{\infty} e^{irap}K_0(|rq_xa|) - \frac{\pi\Gamma}{a}\frac{\eta_-(z_0)}{\eta_+(z_0)}\sum_{n=-\infty}^{\infty}\frac{e^{-2|z_0|\sqrt{(p-2\pi n/a)^2+q_x^2}}}{\sqrt{(p-2\pi n/a)^2+q_x^2}}\right\}. \tag{34}$$

The last sum is periodic under $p \to p \pm \frac{2\pi}{a}$. The $r=0$ term on the right-hand side of Eq. (34) involves Coulombic self-interaction of a wire internally, and its apparent divergence is abated by recognizing that we must consider its small, but finite, width b setting $K_0(0) \to K_0(q_xb)$. With this, we have

$$\sum_{r=-\infty}^{\infty} e^{irap}K_0(|rq_xa|) = K_0(q_xb) + 2\sum_{r=1}^{\infty}\cos(rpa)K_0(|rq_xa|), \tag{35}$$

which is easily approximated for $q_xa \ll 1$.[25] (The case $q_xa > 1$ essentially corresponds to the case of a single wire that is not of interest here.[26]) Furthermore, for low wave number ($m \gg q_xq_F$) we have $\Sigma_{\alpha}R_{\alpha}(q_x,\omega) \to \frac{n_{1D}q_x^2}{m\omega^2}$ where $n_{1D}=\frac{2q_F}{\pi}$ is the one-dimensional (1D) wire electron density per unit length and q_F is the Fermi wave number.

Considering that Eq. (34) is periodic in the reciprocal-lattice wave number, $p \to p \pm 2\pi/a$, it is clear that the plasmon spectrum will involve bands that we will examine in the first Brillouin zone, $\pi/a \leqslant p \leqslant \pi/a$.

V. PLASMON SPECTRA

To start, we consider $\mathbf{z_0} < \mathbf{0}$ with a periodic lattice structure in the nature of quantum wires situated outside the semi-infinite bulk medium, with background dielectric constant $\varepsilon' = 1$. In this case, Eq. (34) becomes

$$1 = \frac{2e^2n_{1D}q_x^2}{m\omega^2}\left[\sum_{r=-\infty}^{\infty} e^{irap}K_0(|rq_xa|) + \frac{\pi}{a}\Gamma\sum_{n=-\infty}^{\infty}\frac{e^{-2|z_0|\sqrt{(p-2n\pi/a)^2+q_x^2}}}{\sqrt{(p-2n\pi/a)^2+q_x^2}}\right], \tag{36}$$

where Γ, the semi-infinite plasma image strength function, is given by

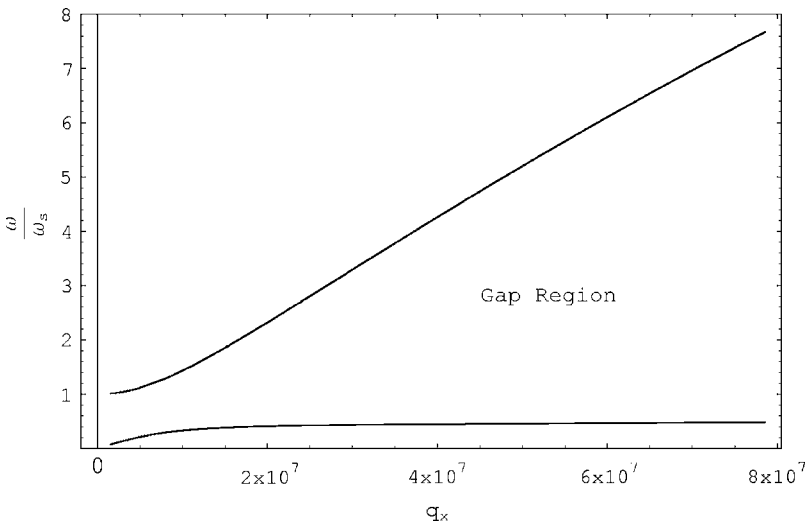

FIG. 4. $\omega_{\pm}/\omega_s$ as functions of q_x (1/m) for $z_0=-1$ nm, $a=10$ nm, $p=10^8/\mathrm{m}$.

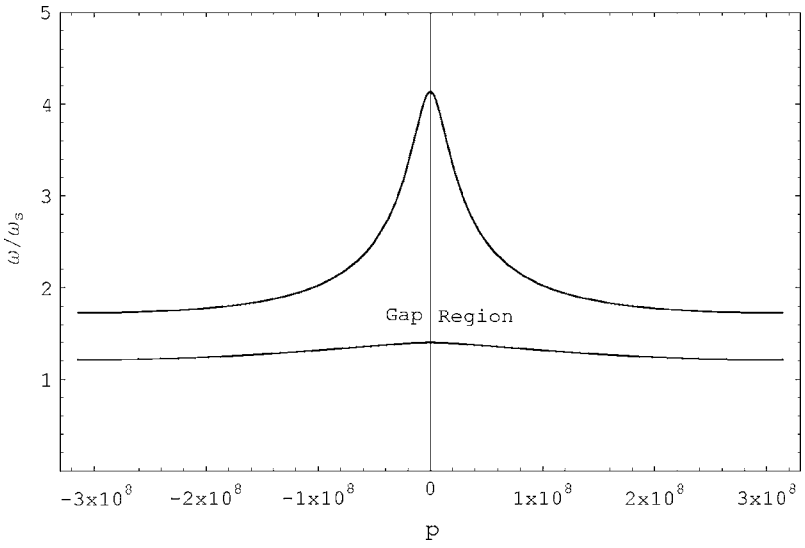

FIG. 5. $\omega_\pm/\omega_s$ as functions of p (1/m) for $z_0=1$ nm, $a=10$ nm, $q_x=0.1q_F$.

$$\Gamma = \frac{\omega_p^2}{2\omega^2 - \omega_p^2}, \tag{37}$$

with ω_p as the classical plasma frequency of the semi-infinite bulk taken in the local limit for illustrative purposes. As Eq. (36) is quadratic in ω^2, it can be solved exactly with the result (subject to $\omega_\pm^2 > 0$),

$$\omega_\pm^2 = \frac{1}{2}\left[AB + \frac{\omega_p^2}{2} \pm \sqrt{A^2B^2 + 2AC - AB\omega_p^2 + \frac{\omega_p^4}{4}}\right], \tag{38}$$

where

$$A = \frac{2e^2 n_{1D} q_x^2}{m}, \tag{39}$$

$$B = \sum_{r=-\infty}^{\infty} e^{irap} K_0(|rq_x a|), \tag{40}$$

$$C = \frac{\pi}{a}\omega_p^2 \sum_{n=-\infty}^{\infty} \frac{e^{-2|z_0|\sqrt{(p-2n\pi/a)^2+q_x^2}}}{\sqrt{(p-2n\pi/a)^2+q_x^2}}. \tag{41}$$

This spectrum contains two bands of plasmon modes in the first Brillouin zone, $-\pi/a \leqslant p \leqslant \pi/a$. The gap separating the two bands may be described in terms of

$$\Delta(\omega^2) \equiv \omega_+^2 - \omega_-^2 = \sqrt{A^2B^2 + 2AC - AB\omega_p^2 + \frac{\omega_p^4}{4}}. \tag{42}$$

These bands and the gap between them are exhibited as functions of p in the first Brillouin zone in Fig. 1 for superlattice period $a=20$ nm with ω normalized to the surface plasmon frequency, $\omega_s=\omega_p/\sqrt{2}$ and $z_0=-1$ nm, $q_x=0.1q_F$ (q_F is the Fermi wave number; $q_F=1.7\times10^8$/m for a 1D quantum wire of density $n_{1D}=10^8$/m).

The dependence of the spectrum on the period a of the quantum wire superlattice is shown in Fig. 2 over the range $0<a\leqslant 200$ nm. The parameters here are $z_0=-1$ nm, $p=4\times10^8$/m, $q_x=0.1q_F$.

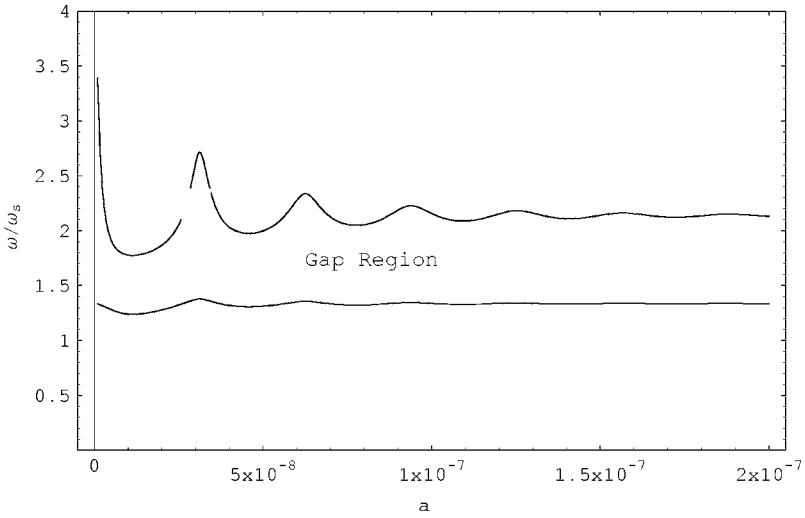

FIG. 6. $\omega_\pm/\omega_s$ as functions of a (m) for $z_0=1$ nm, $p=2\times10^8$/m, $q_x=0.1q_F$.

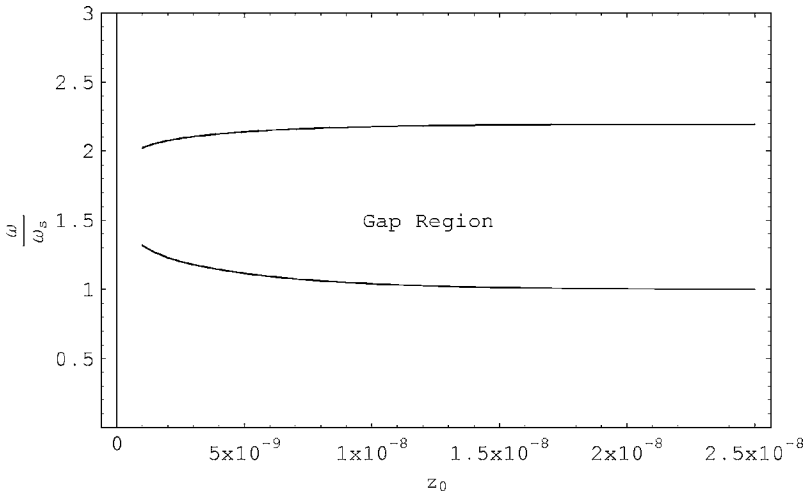

FIG. 7. $\omega_{\pm}/\omega_s$ as functions of positive z_0 (m) for $a=10$ nm, $p=10^8/\mathrm{m}$, $q_x=0.1q_F$.

The spectrum may be seen as a function of negative z_0 in Fig. 3 over the range $0>z_0>-25$ nm, with parameters $a=10$ nm, $p=10^8/\mathrm{m}$, $q_x=0.1q_F$.

The coupled plasmon mode dependence on q_x is exhibited in Fig. 4 over the range $0<q_x<8\times10^7/\mathrm{m}$, with parameters $z_0=-1$ nm, $a=10$ nm, $p=10^8/\mathrm{m}$.

It is, of course, of interest to examine the coupled plasmon spectrum with $\mathbf{z_0}>\mathbf{0}$, so that the quantum wire superlattice is embedded within the semi-infinite bulk plasma medium. In this case the dispersion relation [Eq. (34)] is given by

$$1-\frac{\omega_p^2}{\omega^2}=\frac{A}{\omega^2}\left[B-\frac{C}{2\omega^2-\omega_p^2}\right]. \tag{43}$$

Again, this is a quadratic equation with the solution

$$\omega_{\pm}^2=\frac{1}{2}[AB+\omega_s^2\pm\sqrt{A^2B^2-2AC+AB\omega_p^2+\omega_s^4}], \tag{44}$$

and the spectrum again contains two bands [which differ from those of Eq. (38)] and the gap between them is given by

$$\Delta(\omega^2)=\sqrt{A^2B^2-2AC+AB\omega_p^2+\omega_s^4}. \tag{45}$$

The two bands are exhibited as functions of p in the first Brillouin zone in Fig. 5 for $z_0=1$ nm, wire superlattice period $a=10$ nm, $q_x=0.1q_F$.

The dependence of the spectrum on superlattice period a is shown in Fig. 6 over the range $0<a<200$ nm. The parameters are $z_0=1$ nm, $p=2\times10^8/\mathrm{m}$, $q_x=0.1q_F$. In Fig. 7, the coupled plasmons may be seen as functions of positive z_0 over the range $1<z_0<25$ nm, with parameters $a=10$ nm, $p=10^8/\mathrm{m}$, $q_x=0.1q_F$. Finally, the spectrum as a function of q_x is illustrated in Fig. 8 over the range $0<q_x<8\times10^7/\mathrm{m}$, with parameters $z_0=1$ nm, $a=10$ nm, $p=8\times10^7/\mathrm{m}$.

Coupled plasmonic band structure in the first Brillouin zone is evident in Figs. 1 and 5 for $z_0<0$ and $z_0>0$, respectively, along with the band gaps. Figures 2 and 6 ($z_0<0$ and $z_0>0$) are particularly interesting because the variation of the spectrum (and gaps) clearly reflects on the period of the quantum wire superlattice, opening the possibility of using surface plasmon resonance as a mechanism for optical sensing of nanostructure geometry. Figures 3 and 7 exhibit the dependence of wire-lattice-plasmon coupling to surface plasmons as a function of separation z_0: In Fig. 3 for z_0 negative, it is clear that the lower mode approaches the decoupled

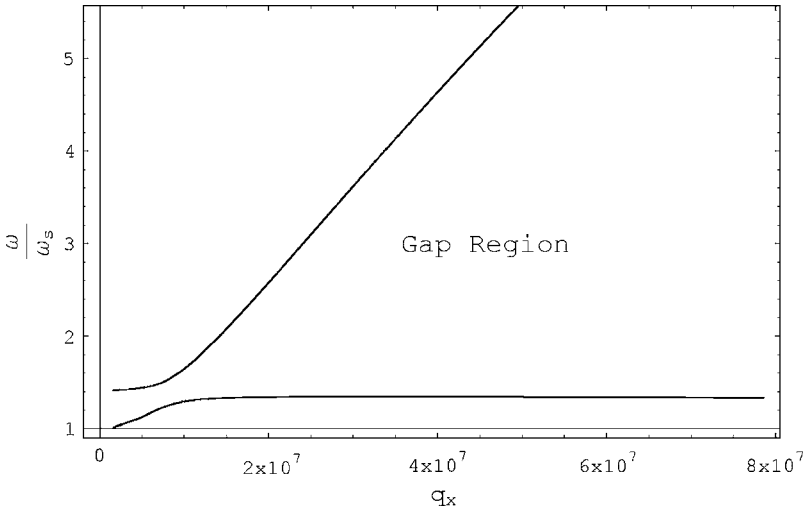

FIG. 8. $\omega_{\pm}/\omega_s$ as functions of q_x (1/m) for $z_0=1$ nm, $a=10$ nm, $p=8\times10^7/\mathrm{m}$.

surface plasmon for $|z_0|$ large (large separation), but that this mode certainly couples to the wire-lattice plasmon for $|z_0|$ small, when the two component subsystems are in close proximity. Again, in Fig. 7, the lower mode simply decouples the surface plasmon from the distant wire-lattice plasmon for $|z_0|$ large, while the upper mode couples the latter to the bulk plasmon deep in the medium. Finally, Figs. 4 and 8 illustrate the mode-mode repulsion as a function of q_x commonly experienced in the "crossover" region of interacting modes.

VI. CONCLUDING REMARKS

We have carried out a fully analytic determination of the dynamic, nonlocal, inhomogeneous screening function of a semi-infinite plasma-like semiconductor in the presence of a lateral quantum wire-like superlattice. This was done by the explicit inversion of the Coulomb coupled system's direct dielectric function viewed as a matrix in its space-time indicies, formulating and solving the associated RPA-type integral equation for the screening function. The coupled surface-plasmon and wire-superlattice spectrum has been fully analyzed, determining its band and gap structure and dispersion. Our results also show that the coupled spectrum provides information about the geometric parameters of the system, the superlattice period a, and z_o, for the case at hand, which could also be applied to a lattice of long, thin, parallel molecules having mobile carriers capable of conduction. Moreover, the technique employed here can also be extended to providing information about the geometric structure of a molecular architecture through its Coulombic interaction in modifying the spectrum of nearby surface plasmons, in addition to reflecting on the normal-mode frequencies of the molecular structure itself. These considerations open the possibility of further enhancing the already fruitful and effective surface plasmon resonance technique that has been employed in real-time biotechnological measurements of the kinetics of label-free biomolecular interactions (DNA, for example) with high sensitivity.[4–16] Furthermore, our results not only provide the coupled plasmon mode spectrum in terms of the frequency poles of the screening function, but its residues at the pole positions also describe the relative excitation amplitudes (oscillator strengths) of the modes.

ACKNOWLEDGMENTS

We gratefully acknowledge support from the U.S. Department of Defense (DAAD Contract No. 19-01-1-0592) through the DURINT program of the Army Research Office and the NIH/MBRS/SCORE program (Grant No. GM008194). We also thank S. Y. Liu for assistance.

[1] R. H. Ritchie, Phys. Rev. **106**, 874 (1957).
[2] E. A. Stern and R. A. Ferrell, Phys. Rev. **111**, 1214 (1958).
[3] H. Raether, in *Physics of Thin Films* (Academic, New York, 1977), Vol. 9, p. 145.
[4] B. Liedberg, C. Nylander, and I. Lundstrom, Sens. Actuators **4**, 299 (1983).
[5] M. Minunni, Spectroscopy (Amsterdam) **17**, 613 (2003).
[6] I. Pockrand, Surf. Sci. **72**, 577 (1978).
[7] S. Szunerits, L. Bouffier, R. Calemczuk, B. Corso, M. Demeunynck, E. Descamps, Y. Defontaine, J.-B. Fiche, E. Fortin, T. Livache, P. Mailley, A. Roget, and E. Vieil, Electroanalysis **17**, 2001 (2005).
[8] C. Nylander, B. Liedberg, and T. Lind, Sens. Actuators **3**, 79 (1982/83).
[9] T. Gregory Drummond, Michael G. Hill, and Jacqueline K. Barton, Nat. Biotechnol. **21**, 1192 (2003).
[10] P. H. Bolívar, M. Nagel, F. Richter, M. Brucherseifer, H. Kurz, A. Bosserhoff, and R. Büttner, Philos. Trans. R. Soc. London, Ser. A **362**, 323 (2003).
[11] Vitali Silin and Anne Plant, Tibtech **15**, 353 (1997).
[12] H. Miyachi, K. Yano, K. Ikebukuro, M. Kono, S. Hoshina, and I. Karube, Anal. Chim. Acta **407**, 1 (2000).
[13] R. Wang, S. Tombelli, M. Minunni, M. M. Spiriti, and M. Mascini, Biosens. Bioelectron. **20**, 967 (2004).
[14] R. Wang, M. Minunni, S. Tombelli, and M. Mascini, Biosens. Bioelectron. **20**, 598 (2004).
[15] E. Giakoumaki, M. Minunni, S. Tombelli, I. E. Tothill, M. Mascini, P. Bogani, and M. Buiatti, Biosens. Bioelectron. **19**, 337 (2003).
[16] A. Kindlund and I. Lundstrom, Sens. Actuators **3**, 63 (1982).
[17] S. Das Sarma and W.-Y. Lai, Phys. Rev. B **32**, 1401 (1985).
[18] Q. Li and S. Das Sarma, Phys. Rev. B **40**, 5860 (1989); **41**, 10268 (1990); **44**, 6277 (1991).
[19] G. Gumbs, D. Huang, and D. Heitmann, Phys. Rev. B **44**, 8084 (1991).
[20] J.-X. Yu and J.-B. Xia, Solid State Commun. **98**, 227 (1996).
[21] N. J. M. Horing, J. Gumbs, and T. Park, Physica B **299**, 165 (2001).
[22] Norman J. Morgenstern Horing, E. Kamen, and H. L. Cui, Phys. Rev. B **32**, 2184 (1985).
[23] N. J. M. Horing, T. Jena, H. L. Cui, and J. D. Mancini, Phys. Rev. B **54**, 2785 (1996).
[24] Norman J. Morgenstern Horing, G. Fiorenza, and H. L. Cui, Phys. Rev. B **31**, 6349 (1985).
[25] A. P. Prudnikov, Yu. A. Brychkov, and O. I. Marichev, *Integrals and Series* (Gordon and Breach, New York, 1998), Vol. 2, p. 363 #2.16.17.1 and p. 698 #5.9.1.4.
[26] N. J. M. Horing and V. Fessatidis, J. Phys.: Condens. Matter **16**, 2215 (2004).